

A Novel Wireless Accelerometer Board for Measuring Low-Frequency and Low-Amplitude Structural Vibration.

Alessandro Sabato, Maria Q. Feng, Yoshio Fukuda, Domenico Luca Carni, *Member IEEE*, and Giancarlo Fortino, *Senior Member IEEE*

Abstract—Structural Health Monitoring (SHM) plays an important role in maintaining system integrity of aging structures and machinery parts. Micro Electro-Mechanical System (MEMS) accelerometers, because of their low cost and small dimensions, have emerged as attractive sensing tools for monitoring structural condition based on changes in structural vibration characteristics. For SHM applications, these sensors need to detect low-amplitude and low-frequency vibrations (microvibrations). Those are not always feasible with the conventional low-cost digital sensor boards. In this study, a novel accelerometer board, named Acceleration Evaluator (ALE), is developed to achieve more accurate wireless vibration measurements using the full bandwidth of the installed MEMS accelerometer by a Voltage-to-Frequency (V/F) converter, instead of conventional Analog-to-Digital Converter (ADC). The effectiveness of the prototype is evaluated through laboratory tests, demonstrating its measurement accuracy comparable to that of wire-based Integral Electronics Piezoelectric (IEPE) accelerometers. Furthermore, ALE performance for SHM purposes are validated by carrying out shaking table tests on the real-size model of a stone pinnacle of the Washington D.C. National Cathedral.

Index Terms—Wireless telemetry, acceleration measurement, MEMS sensors, system design, structural health monitoring application.

I. INTRODUCTION

ADVANCES made in Micro Electro-Mechanical System (MEMS) technologies and wireless data transmission have created new methodologies for vibration measurements of civil and mechanical structures. Wireless technology has already been used for many applications (e.g. habitat monitoring [1, 2], environmental parameters detection [3, 4], healthcare [5, 6] and supply chain management [7]). However, all of them do not require high accuracy measurement and high transmission rate, thus data acquisition is easy to achieve. On the other hand, Structural Health Monitoring (SHM) applications require the capability of handling large amounts of data, high fidelity sensing, and high-speed data sampling. Measurement systems need to be sensitive in a wide range of accelerations ($10^{-2} \text{ m}\cdot\text{s}^{-2}$ to $10^1 \text{ m}\cdot\text{s}^{-2}$) [8, 9] and low-frequencies (10^{-1} to 10^1 Hz) [10, 11]. Since the late 1990s,

This research was part of a Ph.D. program funded at Università della Calabria, Italy by European Union social fund within the POR Calabria FSE 2007 - 2013 project. A. Sabato is now with University of Massachusetts Lowell he was together with D. L. Carni and G. Fortino who are with Università della Calabria, 87036 Rende (CS), Italy. (e-mail: sabatoale@gmail.com; dlcarni@deis.unical.it; giancarlo.fortino@unical.it) M. Q. Feng and Y. Fukuda are with Columbia University, New York City, NY 10025, USA. (e-mail: mqf2101@columbia.edu; yf2290@columbia.edu.)

several accelerometer board prototypes have been developed [12, 13]. The first ones employed low-resolution and high-noise-density MEMS sensors [14] coupled together with 10-bit [15] or 12-bit [16] Analog-Digital Converters (ADCs), which were not suitable for measuring microvibrations [9, 15]. Even as more sensitive accelerometers [17] have been used, measurement accuracy was not improved enough for SHM applications even after more sensitive ADCs were embedded on the boards (e.g. 16-bit) [11]. The limiting factor to measurements' accuracy became the precision of the accelerometer itself and, for this reason, the sensor bandwidth and measurement range were reduced to improve board resolution matching it to that of the embedded ADC [11, 18, 19]. This operation narrows the applicability fields and it limits board usage. Other research based on software technologies has been studied, such as the construction of scalable networks [20], the performances of the network itself [21 - 23] and the creation of embedded algorithms for reducing transmitted data volume [24]. Nevertheless, the solution for the fundamental problem of the sensing accuracy is not been presented.

In this study, to compensate for these problems, the Acceleration Evaluator (ALE) [25], a MEMS accelerometer board, is used to achieve accurate wireless microvibration measurements. The wireless transmission capability resolves the following problems: (i) wire impedance, (ii) triboelectric noise, and (iii) mounting facility. ALE effectiveness for SHM applications, which requires the measurement of microvibration, is verified through extensive laboratory tests. In one of them the MEMS accelerometer board is employed during a shaking table test for evaluating the earthquake-induced vibrations on a stone pinnacle. Results show that ALE detects vibrations with a maximum error of nearly 2% when a comparison with Integral Electronics Piezoelectric (IEPE) accelerometers is performed.

ALE joins several other wireless sensor boards for vibration monitoring, but it introduces some novelties compared to existing systems. The main one consists of using a frequency modulation (FM) approach to improve the measurement accuracy. The feasibility of wireless vibration sensors using the FM technique has been demonstrated in many studies, but all of them mainly focused on the low-frequency response characteristics of the wireless transmission [25 - 27]. On the other hand, this research studies the effects this transmission produces on the measurement accuracy. It shows that matching the selected accelerometer with a Voltage-to-Frequency (V/F) converter achieves a resolution of

$0.19 \cdot 10^{-3} \text{ m} \cdot \text{s}^{-2}$ even without modifying the sensor's features (i.e. amplitude and frequency range).

This paper is organized as follows: after Section II, which describes ALE features, a detailed analysis of the laboratory-based experiments is presented in Section III, together with the results of the earthquake-induced vibration test on the stone pinnacle. A quantitative comparison of ALE with the state-of-the-art MEMS-based sensor is presented in Section IV. Finally, conclusions are drawn and future work is briefly outlined in Section V.

II. THE ACCELERATION EVALUATOR FEATURES

Sensor boards typically include one or more sensing element(s), a computational core unit (microcontroller, ADC, flash memory, etc.), and a radio transmitter for wireless communication [28]. For the ALE design, a top-bottom approach has been employed [29]. Starting from an application instance (i.e. the necessity to monitor microvibrations with more accuracy than other MEMS-based sensor boards), the system platform has been developed using the most functional hardware to achieve this goal, and by refining the circuits based on the completed tests [30].

In order to reduce ALE complexity, power consumption, and to improve analyses accuracy, many components have been delocalized off-board. As shown in Figure 1, the custom-developed transmitter board (powered by a 12 V rechargeable battery) consists of three sections. The first one is the sensing element (i.e. accelerometer), which converts the acceleration quantity in voltage values. The second is the signal conditioning section, which supplies the excitation for the sensor, modulates in frequency the sensing element output, and adapts the signal for the next section. The latter is the Radio Frequency (RF) transmitter that modulates the signal conditioning section output and transmits it.

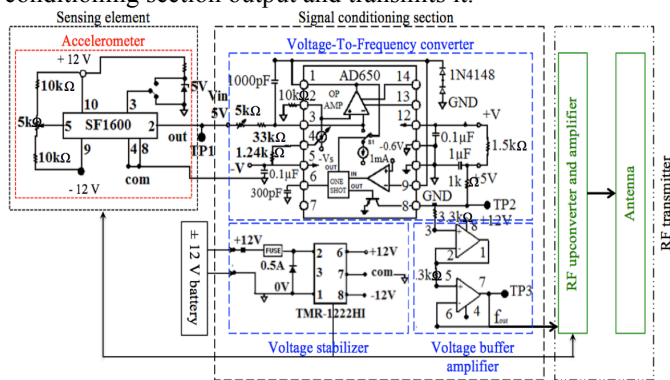


Fig. 1. Hardware diagram of ALE transmitter board

The core components of the three sections are:

- a low floor-noise MEMS-based accelerometer SiFlex 1600SN.A MEMS-based accelerometer SF1600 [31], which can measure an acceleration range of $\pm 29.42 \text{ m} \cdot \text{s}^{-2}$ with a resolution of $0.14 \cdot 10^{-3} \text{ m} \cdot \text{s}^{-2}$ for vibrations from 0 to 1500 Hz;
- a low power V/F converter AD650, which transforms the analog signals measured by the sensor into frequency values minimizing the accuracy loss;

- a low power DC-to-DC converter (TMR3 1222E) used as voltage stabilizer for the sensor board. It prevents from incorrect sensor readings and radio transmission problems which occurs in other systems that do not have a battery voltage up conversion and operate on unregulated battery voltage [9, 32, 33];
- a low power, 4 channels, 2.4 GHz Industrial Scientific and Medical (ISM) RF transmitter for signal transmission to the receiver. Due to limitations highlighted in other publications [25], the RF transmitter is used as a temporary device and the opportunity to substitute it with a more cost-effective will be investigated.

As observed, the board's architecture is simple. The analog sensor output signal is converted to pulses through the V/F converter, which produces a pulse whose frequency is proportional to the signal's voltage value. A proper signal amplifier section for the signal coming out from the V/F is included in the transmitter board shown in Figure 1. This section amplifies the pulse signal before its frequency translation by means of the RF transmitter. It allows solving one of the major issues in vibration data transmission, which is the amplitude-decreasing phenomenon in the low-frequency range. Furthermore, a voltage stabilizer is used to provide a stable power supply to compensate for the gradual decrease in the battery power output over time.

Contrary to many other sensor boards (e.g. [9, 15, 20, 34]), the proposed ALE is equipped with only one sensing element (i.e. SF1600). As shown in Figure 1, the V/F converter is employed instead of an ADC and there are no on-board computational units. By means of the V/F converter it is possible to maximize the accelerometer's performance. The resolution of a 12 V supplied ADC ($9.58 \cdot 10^{-2} \text{ m} \cdot \text{s}^{-2}$ at 10-bit, $2.39 \cdot 10^{-2} \text{ m} \cdot \text{s}^{-2}$ at 12-bit, and $1.50 \cdot 10^{-3} \text{ m} \cdot \text{s}^{-2}$ at 16-bit), would decrease the accuracy due to the resolution of the SF1600. To preserve the selected MEMS accelerometer's resolution performance, a 24-bit ADC ($5.84 \cdot 10^{-6} \text{ m} \cdot \text{s}^{-2}$) should be used, which is too power consuming for low-power wireless systems. For this reason, ALE converts the MEMS sensor output analog signals to FM signals using the V/F converter [35]. Furthermore, to effectively measure microvibrations, it is necessary to overcome the problem arising from the low signal-to-noise ratio output analog signals due to the electrical noise superimposed during the transmission. By converting the analog signal to a FM one, transmission becomes more stable and the robustness against the electrical noise is improved because of modulation characteristics [26]. It is possible to consider the amplitude noise as a perturbation, which affects the signal instantaneous amplitude but leaving the signal's frequency unaltered. Any amplitude variation due to the transmission attenuation can be considered as negligible if the signal strength at the receiver is sufficiently higher than the superimposed noise [36]. In addition, from a circuitual point of view, the amplifier in the transmitter board is not required to be linear because the receiver interprets the frequency variation, only. As a result, the use of a non-linear amplifier permits to increase the energy efficiency of the

communication systems as well [37].

Unlike other sensor controller boards, ALE does not have computational units on it, but demands any computational task to be completed by the receiver. The receiver board down-converts the RF signal in a baseband and demodulates the obtained FM signal. Then, the resulting analog signal is digitalized by a high-resolution Data Acquisition board (DAQ) and post-processed using a Personal Computer (PC). By processing data with the external computer, it becomes possible to treat larger amounts of data and to perform more accurate analyses, which is one of the desirable features in the various engineering sectors. By separating the microcontroller unit (MCU), which takes up a large share of the board's power consumption (between 15 and 25% [20, 22]), total power consumption can be reduced.

In Figure 2 the block scheme of the receiver's three sections is shown. The sections of the receiver board are similar to the transmitter ones with an opposite functionality.

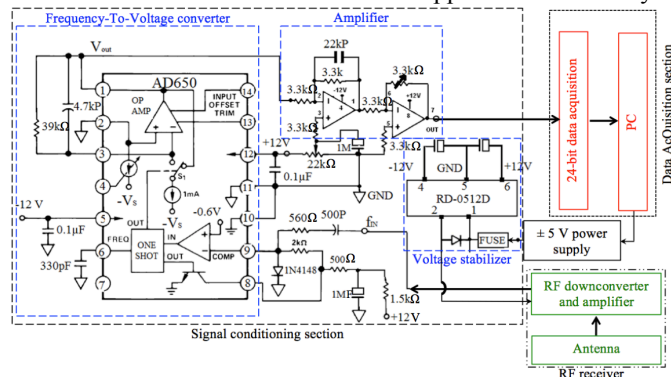


Fig. 2. Hardware diagram of ALE receiver board

The first section is made of a RF receiver, which receives the transmitted signal and down-converts it in a base-band. Successively, the signal conditioning section reconstructs the original analog signal through the Frequency-to-Voltage (F/V) converter. Finally, the data acquisition section uses a 24-bit DAQ to digitalize the reconstructed signal with enough resolution for microvibration detection and to transfer this information to the PC. It manages the acquisition and analyzes the acquired data by using a custom-developed Lab-View code.

III. THE ALE CHARACTERIZATION TESTS

To evaluate ALE performance, several laboratory tests were performed to: (i) demonstrate that ALE accuracy in measuring vibration relevant to SHM applications is comparable with the accuracy of traditionally used wired-based IEPE sensors and (ii) evaluate ALE consistency in measuring microvibrations for civil engineering relevant applications. The first set of experiments referred to stationary signals and the data recorded using ALE were statistically compared with those recorded using an IEPE accelerometer. On the other hand, the second set of tests employed a traditional back-to-back comparison, both in time and frequency domains, with data recorded during a simulated earthquake. Experiments performed for evaluating the

hardware design consistency (i.e. calibration, evaluation of the maximum transmission distance, effect of battery charge) are reported in other research and are not shown here for the sake of brevity [25].

A. ALE Characterization in the Case of Sinusoidal Vibration

Figure 3 shows the test bed for the evaluation of ALE performance in the case of a sinusoidal vibration. The setup is made of an APS 113 shaking table, an IEPE accelerometer (PCB 39B04) as a reference sensor [38], and the ALE transmitter board.

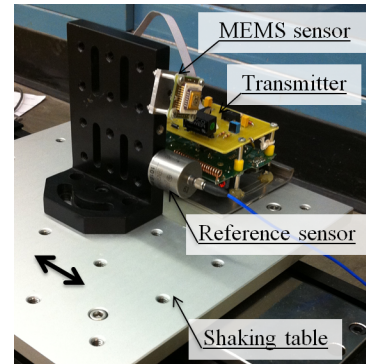


Fig. 3. Test bed for the ALE sinusoidal vibration characterization.

Through this test, ALE sensitivity had been evaluated with low frequency and low amplitude vibrations in a controlled environment. In the test, sinusoidal vibrations with different frequencies (5, 2, 1, 0.5, and 0.2 Hz) and a Root Mean Square (RMS) value of nearly $1.60 \cdot 10^{-2} \text{ m} \cdot \text{s}^{-2}$ (1.63 mg) were used. Lower frequencies and amplitudes were not available because of technical specifications of the shaking table. Both sensors were attached to the shaking table using threaded pin screws, according to the recommendations provided by ISO Standard [39]. For each frequency, a 5-minute measurement at 100 Hz sampling frequency was performed using the ALE receiver, placed 5 meter away from the transmitter board, and the reference sensor.

A statistical analysis was performed evaluating the measured values \bar{x} and their dispersion standard deviation σ . The shaking table supplies a stationary sinusoidal vibration, therefore, each oscillation can be considered as one data set. For instance, when a sinusoidal signal having a period of $T = 0.2 \text{ s}$ (5 Hz oscillation) and a record duration $L = 300 \text{ s}$ is considered, and then the signal is divided into sub-signals with each of them having duration $T = 0.2 \text{ s}$, a total number of $L/T = 1500$ sub-signals (i.e. data set) are generated.

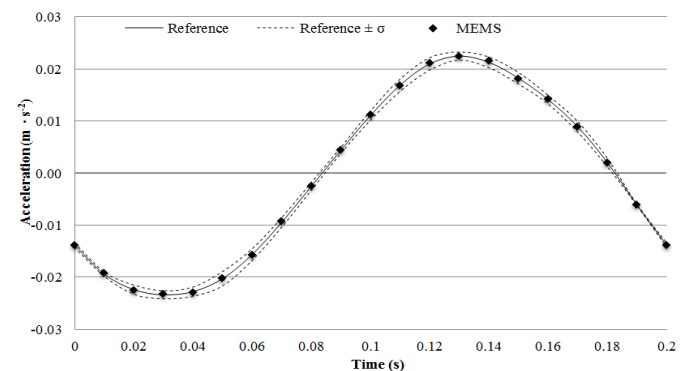


Fig. 4. Reference and MEMS sensors measured values and dispersion (5 Hz)

Considering the 100 Hz sampling rate, each data set consists of 20 sample points. For each of these 20 points, it is possible to evaluate \bar{x} and σ from the 1500 homologous data. Figure 4 shows the trend of the reference sensor results' mean value (continuous line) and the dispersion interval (dashed line) with distance $\pm \sigma$ from the mean value. Figure 4 also plots the results obtained using the ALE (diamond). The results obtained with the two methods are compatible, as it is possible to observe the results obtained with the ALE are always included in the dispersion interval of the reference sensor.

Figure 5 to 9 shows other data plots using the same results for the error comparison by using different acceleration frequencies. In these figures, the dispersion of the data points measured using ALE is normalized to the dispersion of the data points measured using the reference sensor (the data points are shifted using the average values of the reference sensor as a baseline). The intersection between the two intervals (Reference $\pm \sigma$ and MEMS $\pm \sigma$) highlights the compatibility of the results between the two sensors. In particular, the figures show: (i) the dispersion range in which reference sensor's measured values are supposed to be (continuous line and vertical bars representing the reference sensor data dispersion, Reference $\pm \sigma$), (ii) the MEMS sensor's measured values evaluated as difference with the reference sensor measured values (diamonds, which represent the difference Reference - MEMS), (iii) the MEMS data dispersion range (dashed lines, MEMS $\pm \sigma$).

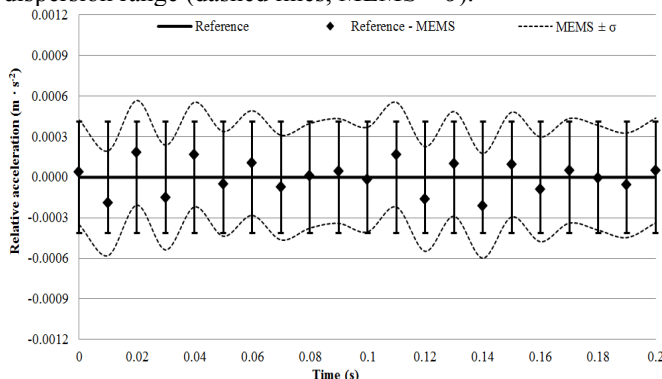


Fig. 5. Error comparison between measurement by ALE and measurement by the reference sensor (5 Hz)

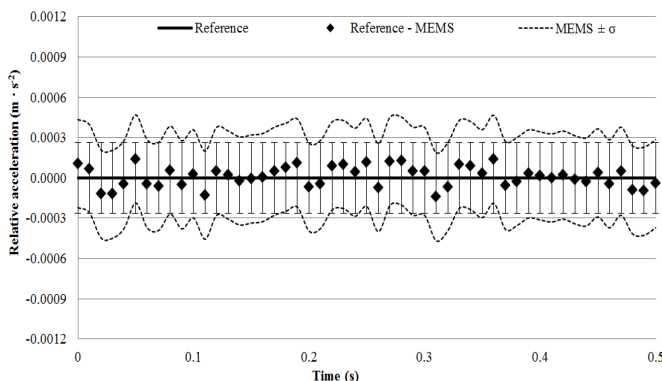


Fig. 6. Error comparison between measurement by ALE and measurement by the reference sensor (2 Hz)

By analyzing the plots, a substantial correspondence is observed in recorded data. The measurement values by ALE

are constantly within the range of the dispersion measured by the reference sensor when frequency is higher than 0.5 Hz.

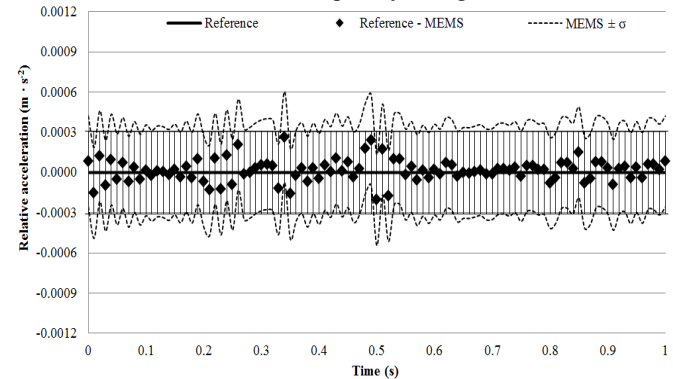


Fig. 7. Error comparison between measurement by ALE and measurement by the reference sensor (1 Hz)

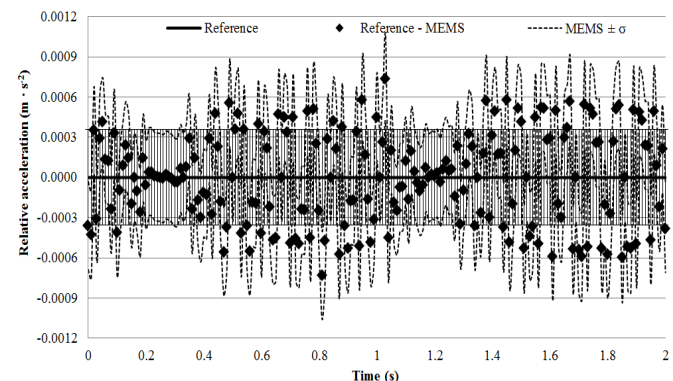


Fig. 8. Error comparison between measurement by ALE and measurement by the reference sensor (0.5 Hz)

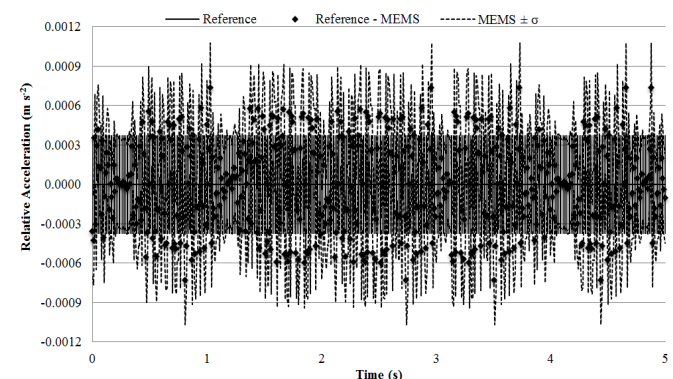


Fig. 9. Error comparison between measurement by ALE and measurement by the reference sensor (0.2 Hz)

For lower frequencies, several measurement values are out of the range. This result demonstrates that measurement errors increase as the frequency of the vibration decreases.

B. Measurement of Structural Seismic Response

Finally, to evaluate the efficacy of ALE in monitoring vibrations of real engineering structures, a shaking table test on an actual structure model had been performed. ALE was used for evaluating the earthquake-induced vibrations on a special lab-scale model of a stone pinnacle, and its performance was compared with that of an IEPE accelerometer PCB 39B04 as a reference. Figure 10 shows a 2,500 kg, 3 m high pinnacle model of the Washington D.C.

National Cathedral, which is placed on an ANCO/MTS Hydraulic 2 Ton shaking table.

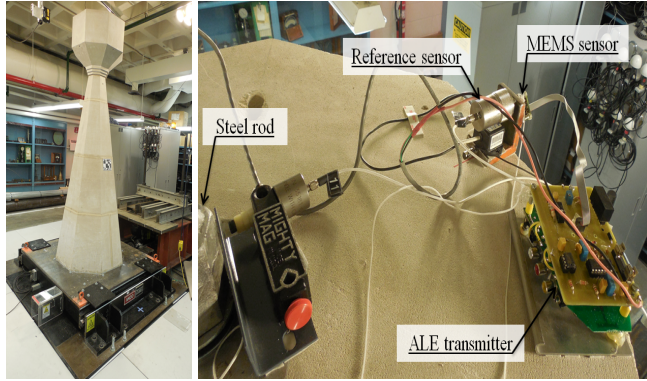


Fig. 10. Pinnacle model (left) and sensors installation (right)

TABLE I
EARTHQUAKE INPUT FEATURES

Duration (s)	PGA ($m \cdot s^{-2}$)	I_A ($m \cdot s^{-1}$)	f_1 (Hz)	f_2 (Hz)	f_3 (Hz)
23.00	1.56	0.21	0.76	1.03	1.61

The features of the simulated seismic vibration (50% of the original record) are listed in Table I. In the table, the Peak Ground Acceleration (PGA), the earthquake's first-three fundamental frequencies f_i , and the Arias Intensity I_A (a measure of the strength of a ground motion of the seismic vibration) are shown [10]. During the test, the vibration was monitored with 100 Hz sampling frequency using an external DAQ system connected to the ALE receiver and the IEPE sensor. Results are plotted in Figures 11 and 12 where the THs recorded with the two sensors at two different times are reported and the structure frequency responses are highlighted.

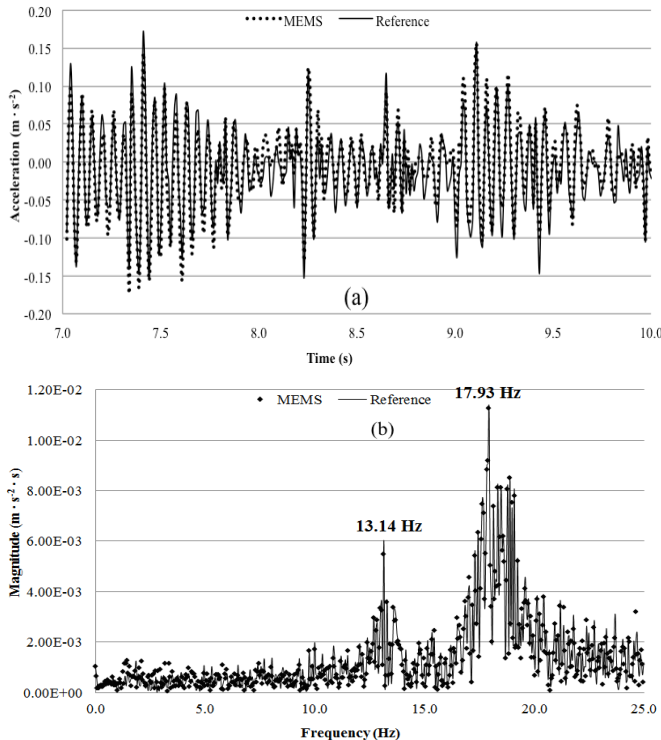


Fig. 11. Comparison of measurements by the two sensors in time domain (a), structural natural frequencies (b) (amplitude range: 10^{-2} - 10^{-1} $m \cdot s^{-2}$)

In particular, Figure 11 refers to vibrations produced by the shaking table's auxiliary machineries (e.g. pump, oil circuit, etc.). They can be considered as ambient vibrations characterized by low-amplitude (10^{-2} - 10^{-1} $m \cdot s^{-2}$) and used for evaluating the natural frequency of the pinnacle (13.14 Hz and 17.93 Hz). Figure 12 refers to the high-amplitude earthquake-induced seismic vibrations (amplitude range: 10^0 $m \cdot s^{-2}$) and it allows the detecting of the characteristic frequencies of both the earthquake (0.77 Hz, 1.03 Hz, and 1.57 Hz) and the pinnacle (17.06 Hz).

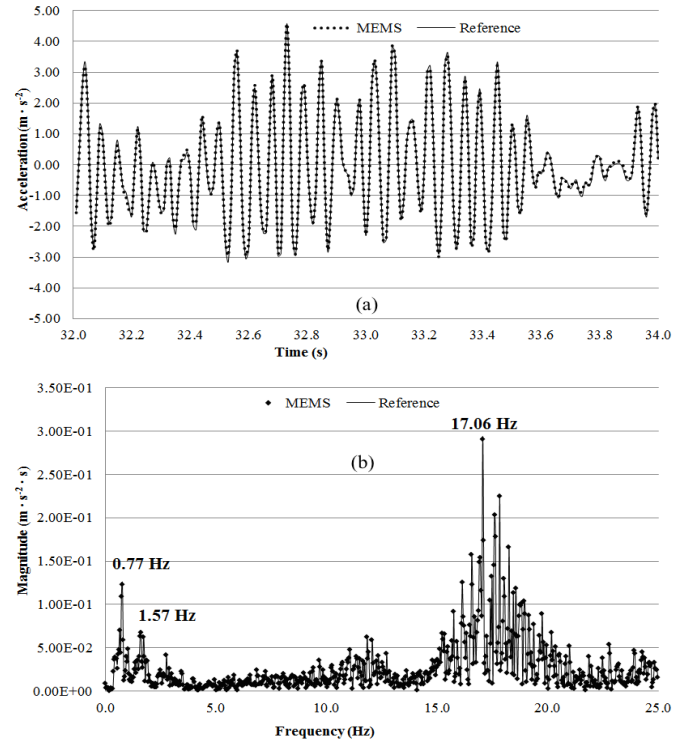


Fig. 12. Comparison of measurements by the two sensors in time domain (a), structural natural frequencies (b) (amplitude range: 10^0 $m \cdot s^{-2}$)

As shown in the figures, an excellent agreement between data recorded with the two sensors is observed. Table II lists a summary of the obtained results, where the I_A , the PGA, and the f_i recorded with the ALE and the reference sensor are numerically compared, and an evaluation of the committed relative error ε is carried out.

TABLE II
SUMMARY RESULTS FOR THE PINNACLE COMPARATIVE TEST

Quantity	MEMS	Reference	ε (%)
PGA ($m \cdot s^{-2}$)	4.518	4.517	0.02
I_A ($m \cdot s^{-1}$)	4.89	4.99	-2.08
f_1 (Hz)	0.77	0.77	0.00
f_2 (Hz)	1.03	1.03	0.00
f_3 (Hz)	1.57	1.57	0.00
f_4 (Hz)	13.14	13.14	0.00
f_5 (Hz)	17.06	17.06	0.00

As can be observed, the PGA and the I_A values are close to each other (relative errors equal to 0.02% and -2.08% respectively). This means that ALE can detect the peak acceleration acting on a system as well as the incident energy, with the same accuracy of a high sensitivity, wire-based, IEPE accelerometer. The frequency domain analyses show the same conclusions as well.

Since the recorded earthquake signal is non-stationary, a time-frequency analysis is performed on both datasets and results are plotted in Figure 13 where no significant differences can be observed in the two plots. In particular, when the central part of the earthquake is considered ($t = 33.12$ s), the two devices report the same value (17.00 Hz) as the fundamental frequency of the stone pinnacle. The error committed on the magnitude, equal to 1.18%, is consistent with the errors reported in the other tests. The small differences in frequency values listed in Table II are due to different integration methods used. Through this test, it is confirmed that ALE has an equal effectiveness to high performance sensors, those usually employed for SHM, even for vibration around 1 Hz.

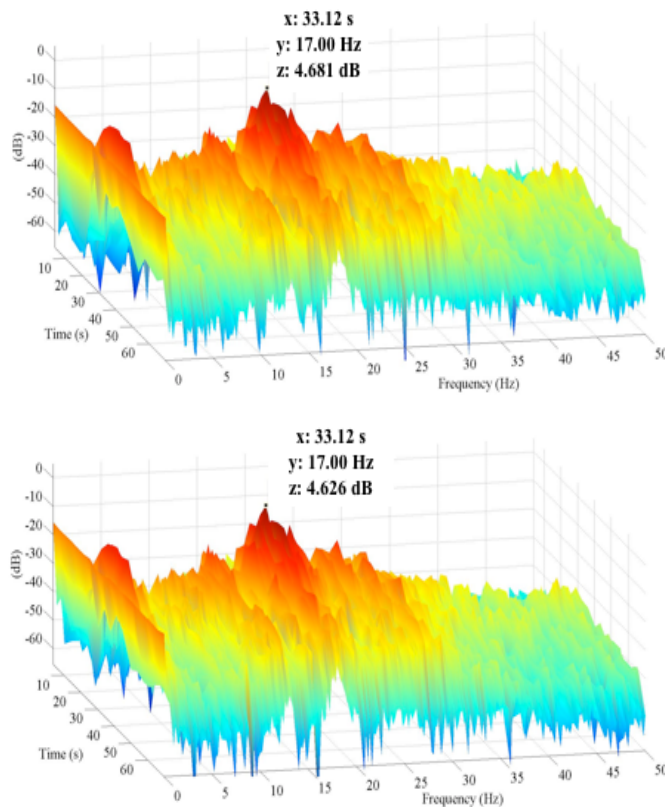


Fig. 13. Comparison of time-frequency analyses of the measurement by ALE (up) and measurement by the reference sensor (down).

Moreover, correspondence in the frequency domain was also confirmed in the earthquake characteristic frequencies (f_1 , f_2 , and f_3), as well as in the natural frequencies of the pinnacle (f_4 and f_5).

IV. RELATED WORKS

ALE has compared with several other academia-built prototypes and commercially available sensor boards for structural vibration detection [13], [40]. Among the most relevant ones, studies published by Kurata et al. [15], Ruiz Sandoval et al. [34], Pakzad et al. [20], and Jo et al. [18], are summarized in Table III and compared with the ALE features. As it is observed in their research, Kurata et al. used a commercially available sensor board embedding a low-cost, high noise-floor level sensor (i.e. ADXL202 [14]) and a 10-bit

ADC, features not suited for SHM. The board only has the capability to detect high-amplitude vibrations. Ruiz-Sandoval et al. improved the same board by using a high-performance accelerometer (SD-1221L [17]), however, due to the 10-bit ADC the resolution is still limited to $23.94 \cdot 10^{-3} \text{ m}\cdot\text{s}^{-2}$ and the system can only detect above 2 Hz frequency vibrations. On the other hand, Pakzad et al. proposed a customized board using the same high-performance with a 16-bit ADC. In this case, the limiting factor to the measurement resolution became the installed sensor ($1.24 \cdot 10^{-3} \text{ m}\cdot\text{s}^{-2}$). For this reason, sensor bandwidth and measurement range were decreased from 400 Hz to 25 Hz and from $\pm 19.61 \text{ m}\cdot\text{s}^{-2}$ to $\pm 0.98 \text{ m}\cdot\text{s}^{-2}$ to improve the sensor's resolution and matching it to that of the embedded ADC ($0.37 \cdot 10^{-3} \text{ m}\cdot\text{s}^{-2}$). Similarly, Jo et al. artificially reduced the sensing range and the bandwidth to achieve a resolution of $0.43 \cdot 10^{-3} \text{ m}\cdot\text{s}^{-2}$ and a lower frequency limit of nearly 1 Hz using a customized design 16-bit ADC.

TABLE III
AVAILABLE SENSOR BOARDS SUMMARY AND COMPARISON WITH ALE

Study	Sensing Range ($\text{m}\cdot\text{s}^{-2}$)	Bandwidth (Hz)	ADC (bit)	ADC Res. ($10^{-3} \text{ m}\cdot\text{s}^{-2}$)	ADC Cons. (mA)	Board Res. ($10^{-3} \text{ m}\cdot\text{s}^{-2}$)
Kurata [15]	± 19.61	5 - 50	10	92.08	9.46	43.85
Ruiz-Sand. [34]	± 19.61	2 - 400	10	23.94	9.46	1.24
Pakzad1 [20]	± 19.61	DC - 400	16	0.37	26.67	1.24
Pakzad2 [20]	± 0.98	0.20 - 25	16	0.37	26.67	0.31
Jo1 [18]	± 19.61	DC - 400	16	0.37	17.40	1.24
Jo2 [18]	± 1.96	1 - 15	16	0.37	17.40	0.43
ALE	± 29.42	0.20 - 1500	-	-	-	0.19

It is possible to observe that using higher resolution ADCs or sensors can improve the measurement accuracy. As highlighted in Table III, an increase in the ADC resolution corresponds to an increase in the power consumption. As stated before, the high-performance MEMS accelerometer selected in this study should be matched with a 24-bit ADC, which demands up to 100 mA for working [41]. This value is extremely exaggerated for low-power wireless systems, especially considering that a comparable measurement accuracy can be obtained using an V/F converter, which power consumption is nearly 10 mA [42].

As listed in the table, ALE achieves superior performance without modification of the accelerometer features. In particular, maintaining a wide bandwidth (0.20 - 1500 Hz) and the full sensing range ($\pm 29.42 \text{ m}\cdot\text{s}^{-2}$), results in the best resolution and the lower detectable frequency are achieved compared with the presented systems. Since no bandwidth reduction is applied, ALE can be used as a multi-purpose device for monitoring systems that have higher vibration frequencies.

V. CONCLUSIONS

In this study, a novel wireless MEMS accelerometer board embedding a V/F converter, is proposed and developed for the purpose of SHM and microvibrations monitoring. This system improves the measurement resolution without modifying and limiting any of the embedded sensor features. It also employs a V/F converter, which creates the Frequency Modulated signals for high-accuracy measurement and low-noise wireless data transmission. Unlike most of the conventional MEMS-

based wireless sensing systems, which have bandwidth limitations to increase measurement accuracy, the developed system does not limit the performance of the embedded MEMS accelerometer. In order to reduce the power consumption and achieve accurate measurements, the computational section is delocalized off-board. In a series of laboratory tests, ALE's capability of measuring microvibrations (frequency up to 0.2 Hz and amplitude in the order of $10^{-2} \text{ m}\cdot\text{s}^{-2}$) was compared with that of IEPE sensors.

In addition, a shaking table test, using a 2,500 kg and 3 m high pinnacle model and the simulated earthquake-induced seismic vibration was conducted. As a result, the detected errors in frequency and time domains (2%) were comparable in size to the wire-based high-performance accelerometers, and ALE's effectiveness for SHM applications was also confirmed.

Using ALE, it becomes possible to develop a monitoring system, which can accurately detect vibration phenomena without interfering, due to the absence of cables, with the functions and architectural features of large-sized aging structures such as churches, monuments, and sculptures. Further developments of the prototype may consist of using the accelerometer board as a sensing node within Wireless Sensor Network [43] by designing a star-type topology first and more complex topologies later. The absence of on-board ADCs may reduce the conversion time-delay and may help if time-synchronizations have to be guaranteed in different nodes of the network.

REFERENCES

- [1] A. Mainwaring, D. Culler, J. Polastre, R. Szewczyk, and J. Anderson, "Wireless sensor networks for habitat monitoring," in *Proc. ACM - WSN4*, Atlanta, GA, 2002, pp. 88-97.
- [2] P. Juang, H. Oki, Y. Wang, M. Martonsi, L.S. Pehand and D. Rubenstein, "Energy-efficient computing for wildlife tracking: design tradeoffs and early experiences with ZebraNet," in *Proc. ASPLOS*, San Jose, CA, 2002, pp. 96-107.
- [3] J. Burrell, T. Brooke, and R. Beckwith, "Vineyard computing: sensor networks in agricultural production," *IEEE Pervasive computing*, vol. 3, no. 1, pp. 38-45, Jan, 2004.
- [4] A. Camilli, C.E. Cugnasca, A.M. Saraiva, A.R. Hirakawa, and P. Correa, "From wireless sensor to field mapping: anatomy of an application for precision agriculture," *Computers and electronics in agriculture*, vol. 58, no. 1, pp. 25-36, Aug, 2007.
- [5] G. Fortino, R. Giannantonio, R. Gravina, P. Kuryloski, and R. Jafari: "Enabling Effective Programming and flexible management of efficient body sensor network applications". *IEEE T. Human-Machine Systems*, vol. 43, no.1, pp. 115-133, Jan, 2013.
- [6] N. Raveendranathan, S. Galzarano, V. Loseu, R. Gravina, R. Giannantonio, M. Sgroi, R. Jafari, and G. Fortino, G., "From Modeling to Implementation of Virtual Sensors in Body Sensor Networks," *Sensors Journal, IEEE*, vol.12, no.3, pp. 583,593, Mar, 2012.
- [7] M. Malinowsky, M. Moskwa, M. Felfmeier, M. Laibowitz, and A.J. Paradiso, "Cargonet: a low-cost micropower sensor node exploiting quasi-passive wakeup for adaptive asynchronous monitoring for exceptional events," in *Proc. SenSys*, Sydney, Australia, 2007, pp. 145-159.
- [8] M. Calebi, "Seismic instrumentation of buildings (with emphasis on federal buildings)," US geological survey, Meno Park, CA, Abbrev. State, Rep. 0-7460-68170, 2002.
- [9] S.D. Glaser, "Some real-world application of wireless sensor nodes," in *Proc. SPIE*, San Diego, CA, 2004, pp. 344-355.
- [10] A.K. Chopra, *Dynamics of Structures: Theory and Applications to Earthquake Engineering*, 4th ed. Prentice Hall, Boston, 2012.
- [11] S. Kim, S.N. Pakzad, D. Culler, J.W. Demmel, G.L. Fennes, S.D. Glaser, and M. Turon, "Health monitoring of civil infrastructures using wireless sensor networks," in *Proc. IEEE - ISPN*, Cambridge, MA, 2007, pp. 254-263.
- [12] S. Gajjar, N. Choksi, M. Sarkar, and K. Dasgupta, "Comparative analysis of wireless sensor network motes," in *IEEE - SPIN*, Noida, India, 2014, pp. 426-431.
- [13] J.P. Lynch, and K.J. Loh, "A summary review of wireless sensors and sensor networks for structural health monitoring," *Shock and Vib. Dig.*, vol. 38, no.2, pp. 91-130, 2006.
- [14] ADXL202/ADXL210: Low Cost $\pm 2g/\pm 10g$ dual axis iMEMS accelerometers with digital output, Available online: <http://www.analog.com> (accessed on Sep. 2014).
- [15] N. Kurata, B.F. Spencer, and M. Ruiz-Sandoval, "Risk monitoring of buildings with wireless sensor networks," *Structural control and health monitoring*, vol. 12, no.3-4, pp. 315-327, Jun, 2005.
- [16] M.J. Whelan, M.V. Gangone, and K.D. Janoyan, "Highway bridge assessment using an adaptive real-time wireless sensor network," *IEEE Sensors Journal*, vol. 9, no. 11, pp. 1405-1413, Nov, 2009
- [17] SD-1221: Low-noise Analog Accelerometer. Available online: <http://www.silicondesigns.com/pdfs/1221.pdf> (accessed on Sep. 2014).
- [18] H. Jo, S. Sim, T. Nagayama, and B.F. Spencer, "Development and Application of High-Sensitivity Wireless Smart Sensors for Decentralized Stochastic Modal Identification," *J Eng. Mech.*, vol. 136, no.6, pp. 683-694, Jun, 2012.
- [19] S. N. Pakzad, "Development and deployment of large scale wireless sensor network on a long-span bridge," *Smart Struct. and Sys.*, vol. 6, no.5-6, pp. 525-543, June, 2010.
- [20] S. N. Pakzad, G.L. Fennes, S. Kim, and D. Culler, "Design and implementation of scalable wireless sensor network for structural monitoring," *J. Infrast. Sys.*, vol. 14, no.1, pp. 89-101, Mar, 2008.
- [21] W. Dargie, "Dynamic power management in wireless sensor networks: state-of-the-art," *IEEE Sens. J.*, vol. 12, no.5, pp. 1518-1528, Apr, 2012.
- [22] A. Sinha, and A. Chandrakasan, "Dynamic power management in wireless sensor networks," *IEEE Des. And Test of Comp.*, vol. 18, no.2, pp. 62-74, Aug, 2001.
- [23] T. Torfs, T. Sterken, S. Brebels, J. Santana, R. van den Hoven, V. Spiering, N. Bertsch, D. Trapani, and D. Zonta, "Low power wireless sensor network for building monitoring," *IEEE Sens. J.*, vol. 13, no.3, pp. 909-915, Jan, 2013.
- [24] L. Dong, and K. Zhang, "Sensing and control of MEMS Accelerometers using Kalman filter," in *Proc. CCDC*, Taiyuan, China, 2012, pp. 3074-3079.
- [25] A. Sabato, and M.Q. Feng, "Feasibility of frequency-modulated wireless transmission for a multi-purpose MEMS-based accelerometer," *Sensors*, vol. 14, no.9, pp. 16563-16585, Sep, 2014.
- [26] D.H. Wang, and W.H. Liao, "Wireless transmission for health monitoring of large structures," *Inst. and Meas., IEEE Trans. on*, vol. 55, no.3, pp. 972-981, Jun, 2006.
- [27] M. Kim, H.S. Yoon, S. Kim, and J.-H. Kim, "Wireless vibration sensor using frequency modulation technique," in *Proc. SPIE*, vol. 8346, pp. 83460-83467, Apr. 2012.
- [28] J.P. Lynch, "Decentralization of wireless monitoring and control technologies for smart civil structures," Ph.D. dissertation, Dept. of Civil and Env. Eng., Stanford Univ., Stanford, CA, 2002.
- [29] A. Sangiovanni-Vincentelli, L. Carloni, F. De Bernardinis, F., and M. Sgroi, "Benefits and challenges for platform-based design," in *Proc. 41st annual Design Automation Conference*, pp. 409-414, June 2004.
- [30] A. Sangiovanni-Vincentelli, and G. Martin, "Platform-based design and software design methodology for embedded systems," *IEEE Design & Test of Computers*, vol. 6, pp. 23-33, June 2001.
- [31] SF1600SN.A: Single axis best in class seismic accelerometer, Available online: <http://www.colibrys.com> (accessed on Apr. 2014).
- [32] M. Leopold, "Sensor Network Motes: Portability and Performance," Ph.D. dissertation, Dept. Computer Science, Københavns Universitet, Copenhagen, Denmark, 2008.
- [33] Ad. Sabato, and Al. Sabato, "Construction and Validation of Small Electro-mechanical Vibration Sensors," *I. J. Comp. Met. and Expe. Meas.*, vol. 1, no.1, pp. 72-79, Jan, 2012.
- [34] M. Ruiz-Sandoval, B.F. Spencer, N. Kurata, "Development of a high sensitivity accelerometer for the Mica platform," in *Proc. IWSHM*, Stanford, CA, 2003, pp. 1027-1035.
- [35] I. Hickman, *Analog Electronic*, 2th ed. Reed Educational, Oxford, MA, 1999.

- [36] B.P. Lathi, *Modern Digital and Analog Communication Systems 3e Osece*, 3rd ed. Oxford University Press, Oxford, 1998.
- [37] S.C. Cripps, *Advanced techniques in RF power amplifier design*, 1st ed. Artech House, London, 2002.
- [38] 393B04: ICP Seismic Accelerometer. Available online: <http://www.pcb.com/products.aspx?m=393C> (accessed on Apr. 2014).
- [39] Mechanical vibration and shock - Mechanical mounting of accelerometers, ISO 5348:2007, 2007.
- [40] J.P. Lynch, "An overview of wireless structural health monitoring for civil structures," *Phil. Trans. Royal Society*, vol. 365, no.1851, pp. 345-372, Feb, 2007.
- [41] AD7760: 2.5 MSPS, 24-Bit, 100 dB. Sigma-Delta ADC, Available online: <http://www.analog.com> (accessed on Nov. 2015).
- [42] AD650 V/F/V voltage-to-frequency or frequency-to-voltage converter, Available online: <http://www.analog.com> (accessed on Nov. 2015).
- [43] G. Fortino, A. Guerrieri, G. M. P. O'Hare, and A. G. Ruzzelli, "A flexible building management framework based on wireless sensor and actuator networks," *J. Network and Computer Applications*, vol. 35, no. 6, pp. 1934-1952, Jun, 2012.



Alessandro Sabato received the B.S. and the M.S. with full marks in environmental engineering and the Ph.D. degree in mechanical engineering from University of Calabria, Italy in 2006, 2010, and 2014, respectively.

He is currently postdoctoral research associate with University of Massachusetts Lowell. He was with Columbia University at the Department

of Civil Engineering and Engineering Mechanics (CEEM) from March 2013 to June 2014 as visiting Ph.D. student and staff-associate from February to June 2014.

His research and work interests include: environmental acoustics, noise and vibration control, wireless MEMS-based technologies, sensor-based structural health monitoring, energy from renewable sources, and HVAC systems. He is author of several publications in these fields.



Maria Q. Feng received the Ph.D. degree in mechanical engineering from the University of Tokyo, Japan in 1992.

She has been Professor of Civil and Environmental Engineering at UC Irvine, from 1992 until 2011, with a joint appointment at the Department of Electrical Engineering and Computer Science. Since January 2012, she joined Columbia University as Renwick

Professor at the Department of Civil Engineering and Engineering Mechanics (CEEM).

Her research interests are primarily in safety and security of civil infrastructure systems, focusing on innovative science and technology for sensors, health monitoring, and damage assessment. She has published near 350 journal and conference proceeding papers on these subjects and she was the recipient of numerous awards and honors.



Yoshio Fukuda was born in Yamaguchi, Japan in 1976. He received the B.S. degree in product system engineering from Ube National College of Technology, Yamaguchi, Japan in 1999 and the M.S. and Ph.D. degrees in mechanical engineering from Nagasaki University, Nagasaki, Japan in 2001 and 2004 respectively.

He is currently an Associate Research Scientist with the Department of Civil Engineering and Engineering Mechanics (CEEM) at Columbia University, New York.

His research interests include visual sensing, man machine interface, human body sensing devices, and civil structure health monitoring.



Domenico Luca Carni achieved the master's degree in Computer Engineering from the University of Calabria, Italy in 2003. In 2006, he received the Ph.D. degree in Systems and Computer Engineering from the same University. At the moment, he is joining the Department of Informatics, Modeling, Electronics and Systems (DIMES), University of Calabria, as

Assistant Professor of Electric and Electronic Measurements. His current research interests include the measurement on telecommunication systems, characterization of digital to analog and analog to digital converters, digital signal processing for monitoring and testing, virtual instrumentation and distributed measurement systems.



Giancarlo Fortino (SM'12) received the Laurea (B.S. and M.S.) and Ph.D. in computer engineering from the University of Calabria, Italy in 1995 and 2000, respectively.

He is currently an Associate Professor of Computer Engineering (since 2006) with the Department of Informatics, Modeling, Electronic and Systems (DIMES), University of Calabria. He holds the

scientific national habilitation for Full Professor and he is also Adjunct Professor of Computer Engineering at the Wuhan University of Technology, China.

He authored over 250 publications in journal, conferences, and books. His research interests include distributed computing, wireless sensor networks, software agents, cloud computing, multimedia networks.